A Collaborative Robotic Approach to Gaze-based Upper-Limb Assisted Reaching

Luca Fortini[1,2], Pietro Balatti[1,3], Edoardo Lamon[1,3], Elena De Momi[2], and Arash Ajoudani[1]

***Abstract*—Robotic treatment has been recognized as a powerful tool to face the consequences of neurological impairments such as stroke. Among several potential benefits, the possibility to program high-intensity and repetitive movements increased the popularity of this type of rehabilitation technologies for upper limb disabilities. Nevertheless, although the results are encouraging, we are still far from guaranteeing a complete recovery to all patients, and some degree of external assistance is required to enable them to execute their activities of daily living. Hence, we aim to build a system which may serve not only as a rehabilitative tool, but also as a complement to assist the users in everyday tasks. In this direction, we present a novel Human-Robot Interface (HRI), which can detect and learn repetitive user movements through gaze, and provide assistance via a collaborative robot. The robot, which provides support to the user's wrist using a comfortable interface, executes the learnt trajectories, enabling the user to perform repetitive movements with reduced effort. The experiments are carried out on ten healthy subjects. We demonstrate that the proposed HRI is not only flexible and intuitive, but also accurate in guiding the users' limb to the desired positions.**

I. Introduction

According to the World Health Organization, 15 million people worldwide suffer from stroke each year, out of which, 5 million lose their lives, and other 5 million become permanently disabled [1]. This has made stroke a leading cause of adult disability. As a consequence, more than half of all stroke survivors depend on caregivers for daily activities [2].

Life-long physical impairment is not limited to stroke patients. Every year, around the world, between 250000 and 500000 people suffer spinal cord injuries (SCI). Common manifestations of upper extremity motor impairment include muscle weakness or contracture, changes in muscle tone, joint laxity, and impaired motor control. These impairments induce disabilities in common activities such as reaching, picking up objects, and holding onto objects [3].

Despite advances in methods of prevention and rehabilitation associated with the disability-causing conditions, a large portion of the world population continues to live with some degree of upper limb physical impairment. For instance, focusing on the stroke upper-limb paresis, functional outcome changes significantly accordingly to the severity of the case. Positive prognosis statistics drop from 71% in mild cases to 5% in acute ones [3]. While devising better rehabilitation methods is a crucial endeavor, it is also important to acknowledge that many people need an alternative form of assistance for physical impairments to regain, at least partially, some sort of independence.

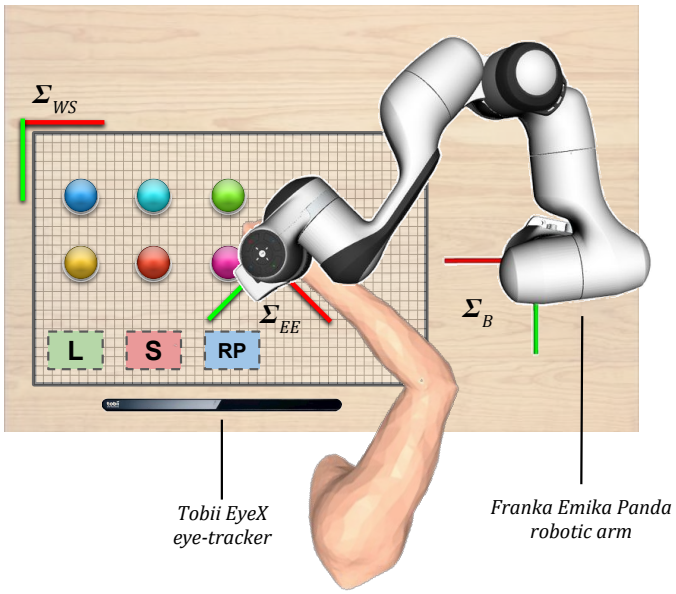

Fig. 1. The upper limb is linked to the end-effector of the robot manipulator which provides gravitational support and active motion triggered by gaze fixation points. At the bottom three gaze-interaction buttons allow the user to access respectively the Learning Phase (L), Stop (S) and Resting Position (RP). Three coordinate reference systems are highlighted: robot base-frame (Σ_B), workspace coordinate System (Σ_{WS}), and robot end-effector reference system (Σ_{EE}).

Reaching-to-grasp is a crucial action in everyday life, allowing the individuals to interact with objects in the environment. It has been proven that this type of action is one of the most frequently used, making it the most worthy to recover [4]. Robot-assisted reaching has been explored widely in the rehabilitation context. Many devices, as MIT-MANUS [5] and the WREX family of robots [6], have proven their effectiveness in tailoring the therapy to the user's needs. However, none of these systems assure the freedom of use and the flexibility required by an unsupervised everyday assisting device. Recently, many studies focused on the identification and interpretation of motion intention in order to guarantee usability and autonomy to the subject. Control methods are countless and are usually based and tailored specifically on the user's residual functional capabilities [7]. In [8], a Motor Imagery based Brain Computer Interface (MI-BCI) has been chosen as a trigger for robotic-assisted movement execution. However, the complexity in decoding the brain signals (electroencephalography) has made their applications limited to the laboratory settings and not

[1]HRI[2] Lab, Dept. of Advanced Robotics, Istituto Italiano di Tecnologia, Genova, Italy. luca.fortini@iit.it
[2]Dept. of Electronics, Information and Bioengineering, Politecnico di Milano, Milano, Italy.
[3]Dept. of Information Engineering, University of Pisa, Pisa, Italy.

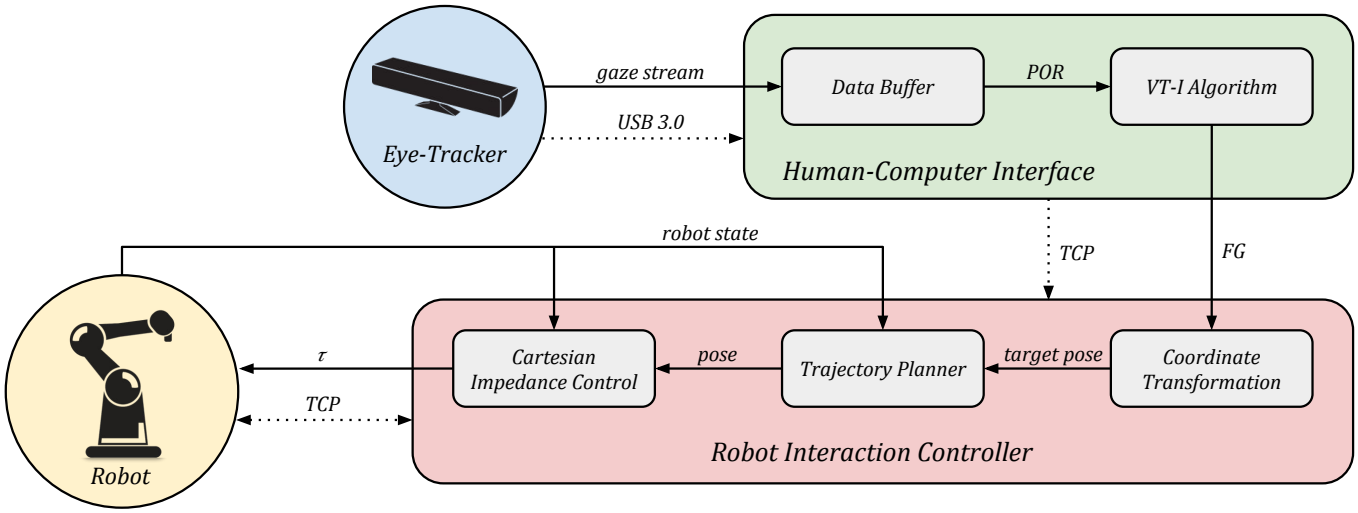

Fig. 2. The Human-Computer Interface buffers the data stream and extracts the relevant information to detect the fixation groups, that, once transposed in the robot reference frame, trigger the trajectory planner which schedules and starts the movement of the robot's end-effector.

ready for the take-up in realistic environments. Additionally, several speech recognition and vocal command systems have been developed and embedded in assistive devices as in [9]. Such option is more suitable for activating discrete actions (e.g., stop, start), whereas in a continuous control case may result in user's frustration and discomfort. On the other hand, vision has established itself as one of the most effective inputs, given its natural role in planning and monitoring the actions in the interaction space. This is the case of devices such as IARUL (Intention-based Assistive Robot for Upper Limb), a gaze-controlled mechanical reaching system [10], and the 3D gaze intention-based grasping support presented in [11].

The increasing interest in eye-tracking based devices is further encouraged by the improvements in accuracy and affordability lately registered. Accordingly, the aim of this paper is to present a robotic assistive-reaching system, to guide the user to reach several target points in the workspace using a commercial eye-tracking system to detect his/her intentions. However, for prolonged activities eye-tracking can be cognitively demanding, hence, we decided to add a learning feature in order to automatize those movements which are classified as repetitive. This feature can be activated or deactivated, simply by looking at predefined virtual switches in the workspace (see Fig. 1).

The assistance is provided by a collaborative robot, holding the user's wrist, and executing the learnt (repetitive) intention-driven trajectories in the workspace. A Cartesian impedance controller is developed with preset gains to guarantee safety. Meanwhile, it ensures that the robot end-effector does no deviate from the desired path, which is due to the gravitational loading introduced by the user's arm weight.

We demonstrate the potential of the proposed gaze-based assistive robotic system in experiments with 10 healthy subjects. Results suggest that the proposed HRI enables the users to intuitively and accurately perform reaching tasks in the workspace, with a significantly reduced physical effort. The latter is demonstrated by the electromyography measurements of the arm muscles in two different conditions: free movements (no robot support is provided), and gaze-based assistance. A task-load questionnaire has been proposed to the subjects to evaluate a third trial which envisages the use of the aforementioned learning interface. The analysis of the answers show a drop in the frustration index performing repetitive duties.

The rest of the paper is organized as follows. Sec. II introduces the proposed HRI. Sec. III explains the experimental setup and specifies the communication protocol implemented in ROS. In the last Section, we discuss the results and highlight future improvements.

II. Method

The aim of the study is to create a robotic system whose movements can be planned and guided using 2D gaze patterns.

A. Human-Computer Interface

Eye tracking refers to the process of measuring where we look, also known as our point of gaze. These measurements are carried out by an eye tracker, that records the position of the eyes and the movements they make. There are several techniques to detect and track eye movements [12]. However, when it comes to remote, nonintrusive, eye tracking the most commonly used technique is Pupil Centre Corneal Reflection (PCCR). The basic concept is to use a light source to illuminate the eye causing highly visible reflections, and a camera to capture an image of the eye showing these reflections. Specific image processing algorithms calculate the eyes position and gaze point analyzing specific details in these reflection patterns.

Gaze space exploration is a combination of steady fixations and rapid eye movements called saccades. A saccade is responsible for rapid movement of the fovea from one point of interest to another, while fixation is the time spent lingering

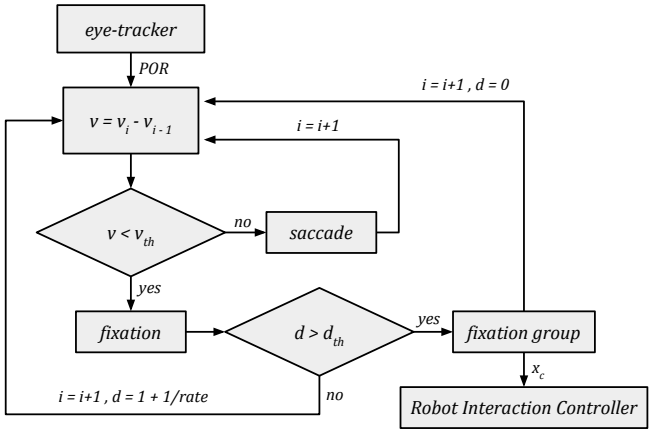

Fig. 3. "Velocity-Threshold Identification Algorithm" - Gaze stream coordinates are classified as fixation points or as saccades using point-to-point velocities as a labeling criterion. Consecutive fixation points are clustered in fixation groups, if maintained for a time-set as a duration threshold.

on these points. Even though, on average, fixations last only $250\,ms$, this time is enough to create a high quality image on the retina allowing details identification and analysis.

From the gaze plots analysis, it can be argued that these movements are not random but underlie valuable information regarding a person's interest and intentions, representing the ideal instrument for human-computer interfaces [13].

Fixations are the most common features extracted to predict intent from gaze data stream. Planar eye-tracking devices return raw data grouped in tuples (x_i, y_i, t_i), where x_i and y_i, known as Points of Regard (POR), represent the gaze coordinates in the work space at time t_i [14].

Some kind of fixation identifier is required to make inferences about reaching intention. Fixation identification has a twofold role: reduce the volume of raw saccades data by collapsing them into more representative tuples, and get rid of noisy aspects as drifts and oscillations which may occur during fixation and result irrelevant for most application [15].

It must be clear that, fixations are not real in the sense of being directly measurable. Fixations are constructions, outputs of a mathematical algorithm that translates the sequence of raw gaze points into an associated sequence of fixations and may differ according to the fixation filter elected.

In this work, a velocity threshold identification (VT-I) algorithm is chosen among those presented in [15] because it matches real-time application requirements. This protocol is built on the definition-based point-to-point velocity gradient between saccades and fixations. Basically, it is possible to distinguish low velocities for fixations (i.e., $< 100\,deg/sec$) and high velocities (i.e., $> 300\,deg/sec$) for saccades. This feature makes velocity-based discrimination fairly fast-implementable and robust.

At every control loop iteration, velocity v is computed as the distance between the current point and the previous one, divided by the control loop sample time. The velocity threshold v_{th} is the eye-movement classification condition. If the fixation condition keeps being true, a collapse process of consecutive fixation points occurs outputting a unique tuple $x_c = (x, y)$ given by the centroid (i.e. Center of Mass) of the consecutive fixation points [15].

Finding the optimal dwell time and velocity threshold is not trivial and it always comes with a trade-off. Interaction may seem unnatural if dwell time increases and, on the other hand, fast interaction may lead to unintentional activations [16]. This problem is known as the Midas touch problem. Moreover, a high velocity threshold comes with a reduction in accuracy, whereas its reduction may boost the cognitive load.

B. Robot Interaction Controller

To achieve safer physical interactions between humans and cobots, it is preferable to employ torque controlled robots with a lightweight structure. In this way, it is possible to plan for robot interactions at the end-effector to perform the primary task, and achieve a suitable null-space behaviour to execute lower hierarchy tasks, e.g., to safely treat the accidental collisions. Hence, for our setup we used a torque-controlled manipulator and designed a Cartesian impedance controller as follows. The vector of robot joint torques $\boldsymbol{\tau} \in \mathbb{R}^n$ is generated as follows:

$$\boldsymbol{\tau} = \boldsymbol{M}(\boldsymbol{q})\ddot{\boldsymbol{q}} + \boldsymbol{C}(\boldsymbol{q}, \dot{\boldsymbol{q}})\dot{\boldsymbol{q}} + \boldsymbol{g}(\boldsymbol{q}) + \boldsymbol{\tau}_{ext}, \tag{1}$$

$$\boldsymbol{\tau}_{ext} = \boldsymbol{J}(\boldsymbol{q})^T \boldsymbol{F}_c + \boldsymbol{\tau}_{st}, \tag{2}$$

where n is the number of joints, $\boldsymbol{q} \in \mathbb{R}^n$ is the joint angles vector, $\boldsymbol{J} \in \mathbb{R}^{6\times n}$ is the robot arm Jacobian matrix, $\boldsymbol{M} \in \mathbb{R}^{n\times n}$ is the mass matrix, $\boldsymbol{C} \in \mathbb{R}^{n\times n}$ is the Coriolis and centrifugal matrix, $\boldsymbol{g} \in \mathbb{R}^n$ is the gravity vector and $\boldsymbol{\tau}_{ext}$ is the external torque vector. $\boldsymbol{F}_c$ represents the forces vector in the Cartesian space and $\boldsymbol{\tau_{st}}$ the second task torques projected onto the null-space of $\boldsymbol{J}$.

Forces $\boldsymbol{F}_c \in \mathbb{R}^6$ are calculated as follows:

$$\boldsymbol{F}_c = \boldsymbol{K}_c(\boldsymbol{X}_d - \boldsymbol{X}_a) + \boldsymbol{D}_c(\dot{\boldsymbol{X}}_d - \dot{\boldsymbol{X}}_a) \tag{3}$$

where $\boldsymbol{K}_c \in \mathbb{R}^{6\times 6}$ and $\boldsymbol{D}_c \in \mathbb{R}^{6\times 6}$ represent respectively the Cartesian stiffness and damping matrix, $\boldsymbol{X}_d$ and $\boldsymbol{X}_a \in \mathbb{R}^6$ the Cartesian desired and actual position, $\dot{\boldsymbol{X}}_d$ and $\dot{\boldsymbol{X}}_d \in \mathbb{R}^6$ their corresponding velocity profiles. The Cartesian desired position and velocity are generated with a fifth-order polynomial trajectory to avoid impulsive jerks and achieve smoother robot movements.

The damping matrix $\boldsymbol{D_c}$ is derived from $\boldsymbol{K}_c$ by:

$$\boldsymbol{D_c} = \boldsymbol{\Lambda}_* \boldsymbol{D}_{diag} \boldsymbol{K}_{adj*} + \boldsymbol{K}_{adj*} \boldsymbol{D}_{diag} \boldsymbol{\Lambda}_*, \tag{4}$$

where $\boldsymbol{D}_{diag}$ is the diagonal matrix containing the damping factor ($\zeta = 0.7$), $\boldsymbol{K}_{adj*}\boldsymbol{K}_{adj*} = \boldsymbol{K}_c$ and $\boldsymbol{\Lambda}_*\boldsymbol{\Lambda}_* = \boldsymbol{\Lambda}$, where $\boldsymbol{\Lambda}$ is the desired end-effector mass matrix [17].

All gaze data are mapped into a 2D coordinate system aligned with the workspace Σ_{WS}. The origin of Σ_{WS} is positioned in the upper left corner of the workspace (Fig. 1). In order to allow the trajectory planner to program the end-effector's path properly, the i-th fixation group (FG_i) should

be represented w.r.t. the robot base reference system Σ_B (Fig. 1), and is computed as follows:

$$\boldsymbol{FG_i}^B = \boldsymbol{T}^B_{WS} \boldsymbol{FG_i}^{WS}, \tag{5}$$

where ${FG_i}^B$ and ${FG_i}^{WS}$ represent, respectively, the i-th fixation group w.r.t. Σ_B and Σ_{WS}, and $\boldsymbol{T}^B_{WS}$ is the transformation between from Σ_{WS} to Σ_B.

At every control loop iteration, the robot compares the position of its end-effector with the last fixation group set as target pose. When these values differ, the memorization of a new target pose is inhibited.

III. Experiments

To show the validity of the presented method, we performed experiments on 10 healthy subjects of different gender, 6 males and 4 females, between 20 and 30 years old. None of the subjects was familiar with eye-tracking technology. Since wearing glasses may cause a drop in accuracy, we tested the tracking robustness of our system by including 4 people wearing them.

A. Setup

The subjects were asked to sit in front of a rectangular workspace with the right hand attached to the robotic arm placed on their right side Fig. 1. The connection between the robot end-effector and the human wrist was realized with a velcro strap, to allow the user to safely detach his/her hand from the robot in case of an emergency. The eye-tracker was positioned at the bottom of the workspace. A led illuminated push-button panel (Fig. 1) was and positioned in the eye-tracked area to simulate reaching tasks, and to assess the reaching performance and the timing. As shown in Fig. 1, three buttons are mapped at the bottom of the pixel matrix of the workspace:

- Learning (L) - When selected the first time, it triggers the recording of an array of gaze poses. To interrupt the learning phase, it is necessary to linger again on this button. Once learned the desired positions the robot automatically moves through the sequence.
- Stop (S) - Puts and end to the loop recorded by means of the "L" button.
- Resting Position (RP) - This feature has been added to get out of situations in which the robot occlude the field of vision. Once triggered, it automatically brings the arm in a more comfortable position, i.e. on the right side of the workspace.

Since these buttons don't provide an haptic feedback a speaker is embedded to be sure of the selection.

The study was performed using a Tobii EyeX, a commercial, entry-level, low-cost ($< 200\,\$$) eye tracker.

Better results can be obtained using 3D wearable high-performance research devices that ensure tracking on all Cartesian axes, and higher accuracy. However remote eye-gaze-trackers guarantee a faster setup and higher comfort of use. Calibration is performed collecting eye-gaze data provided by a calibration routine for a 2D computer screen built-in to the driver. Although EyeX eye-tracker is a screen-based eye tracking system, it is possible to track physical display areas, if the geometrical calibration constraints are respected. During the calibration procedure, the subjects focus the gaze on different points for a few seconds, the time requested by the device to record high-frame-rate images of the reflection patterns of the eyes generated by the near infrared lights. Unlike most "research-grade" eye tracking systems which perform an internal bufferization of the data, the EyeX model can't directly interface with softwares as MATLAB. To accomplish this coupling and query the data coming from the eye-tracker at will, we used Myex, a specifically designed Matlab interface [18].

We conducted experiments using a Franka Emika Panda, a 7 Degrees of Freedom, torque-controlled, lightweight robotic arm specifically intended to share the workspace with humans.

The different devices are integrated and interconnected through the Robot Operating System (ROS) environment [19].

B. Experimental Flow

The lights of the buttons were illuminated sequentially to guide the user through different reaching patterns, while the switches allowed to record timing and success rate of the task. Every subject was asked to replicate the same pattern in three subroutines.

In the first trial the subject had to complete the experiment without the help of the robot. In this way, it was possible to obtain a solid benchmark for the EMG data (see Sec. III-D).

In the second one, the gravitational forces of the arm were supported by the manipulator, leaving to the subject only the eye-gaze trajectory planning to move from one point to the next. It is important to clarify that, in the button lightning schedule, there were some recurrent sequences. In the last trial, the subjects were asked again to follow the button lightening path sustained by the robot, but once identified the aforementioned sequences, he/she could use the learning procedure to automate the trajectories, so as to reduce the eye focusing load.

C. Questionnaire

Quantitative data collected during the experiments were compared with the subjective evaluation of the users. The subjects were asked to rate their workload awareness on a 20-point Likert scale questionnaire based on NASA Task Load Index (Nasa-TLX). This assessment tool derives an overall workload score based on an average of ratings on six subscales:

- Mental Demand (MD)
- Physical Demand (PD)
- Temporal Demand (TD)
- Performance (P)
- Effort (E)
- Frustration (F)

Subjects were asked to fill in the questionnaire after subroutine 2 and 3. The lower an index is, the more demanding (worse performing) the user finds the task [20]. The ratings are

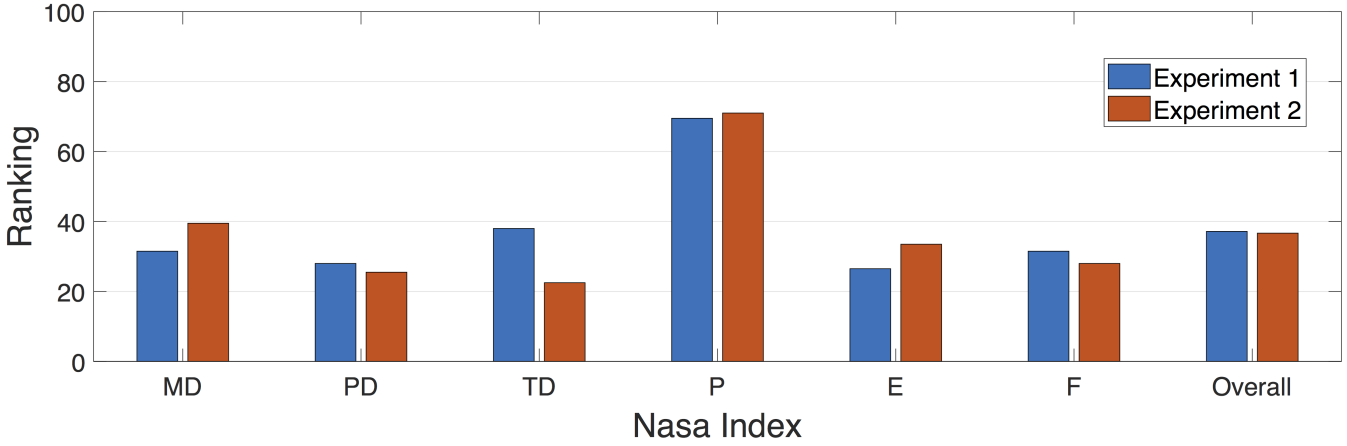

Fig. 4. Nasa-Index Task-load indexes magnitude results. The comparison is performed between the two robot-assisted trials. In blue is shown the subroutine performed without using the learning features while in red the user is free to use them. Mental Demand (MD), Physical Demand (PD), Temporal Demand (TD), Performance (P), Effort (E), Frustration (F).

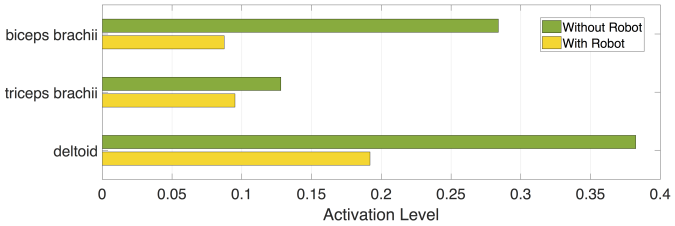

Fig. 5. Comparison between EMG global muscular activity in subroutine 1 without the robot and subroutine 2 with the robot.

then averaged and added to create an estimate of the overall workload.

D. EMG data collection and analysis

Since the experiment was carried out on healthy subjects, surface EMG data were collected during the whole experiment to prove the effectiveness of the gravitational support, and to make a comparison with the answers of the questionnaire. The 2D planar reaching task is a combination of shoulder adduction-abduction and elbow flexion-extension. For this reasons only 3 EMG channels where measured: on the deltoid, on the biceps brachii and on triceps brachii. The EMG signal processing included the analysis of the Root Mean Square value. This parameter is frequently chosen since it reflects the level of the physiological activities in the motor unit during contraction, giving an estimation of the muscular intensity [21]. The data have been normalized w.r.t. the Maximum Voluntary Contraction value among the experiment and averaged to extract some kind of indicator of the overall muscle activity.

IV. Results

The results of the questionnaire are summarized in Fig. 4. All the users were able to complete the task successfully without too much effort, as it can be noticed by the high value of the performance parameter (P). We believe this is due to the great accuracy of the system experienced by the subjects, i.e. the average difference between the location of the button and the eye-gaze guided robot's end-effector position. Even though the experiment was performed on unimpaired subjects they were asked to relax as much as possible and let the robot to compensate for gravity and take care of upper limb movement. Fig. 5 shows a global decrease in muscular activity confirmed also by the low values of Physical Demand (PD) in Fig. 4. The residual activity is probably due to involuntary co-contractions by the users. We can notice that the perceived temporal demand (TD) datum is almost halved. This trend is supported by the averaged measured runtime of the subroutines, approximately 313 s in experiment 1 and 247 s in experiment 2. We believe there is a trade-off between the drop in frustration (F) due to repeating the same tasks several times and the mental demand (MD) and effort (E) spent to identify them and interact with the learning interface.

The overall ranking does not seem to be affected much. The reason can be found in the relative brevity of the task proposed to the subjects.

V. Conclusion

In this paper, we presented a robotic system for reaching assistance. The main objective of the work was to realize a non-invasive setup, that was easy to learn and to use. The control scheme, based on eye-gaze fixations, was implemented and tuned in such a way that no training, detailed instructions, or physical skills was required.

However, the system still needs some developments to fully mimic the natural movements of non-disable subjects. The first limitation is primarily due to the restriction to 2D motion in the horizontal plane. This problem is closely related to the restricted geometrical range of detectable gaze data performed by the selected eye tracker. To enlarge the workspace, without switching to more expensive eye-tracking glasses, it would be necessary to integrate more eye trackers to work simultaneously. However, the Tobii EyeX is not currently compatible

with multiple eye-trackers, since each could interfere with the infrared reflections of the others.

The whole systems targets reaching tasks but it does not face all gestures associated with it such as grasping. It is likely that the subject is not capable of grasping an object, if unable to move the arm to reach it. For this reason some kind of grasping support may be embedded to the system in future works.

Finally, although the prototype behaved well for healthy people, it would be interesting to investigate the effectiveness of the setup when used by individuals with impaired limbs.

REFERENCES

[1] W. H. Organization, *The world health report 2002: reducing risks, promoting healthy life*. World Health Organization, 2002.

[2] J. Adamson, A. Beswick, and S. Ebrahim, "Is stroke the most common cause of disability?" *Journal of stroke and cerebrovascular diseases*, vol. 13, no. 4, pp. 171–177, 2004.

[3] S. M. Hatem, G. Saussez, M. della Faille, V. Prist, X. Zhang, D. Dispa, and Y. Bleyenheuft, "Rehabilitation of motor function after stroke: a multiple systematic review focused on techniques to stimulate upper extremity recovery," *Frontiers in human neuroscience*, vol. 10, p. 442, 2016.

[4] S. L. Kilbreath and R. C. Heard, "Frequency of hand use in healthy older persons," *Australian Journal of Physiotherapy*, vol. 51, no. 2, pp. 119–122, 2005.

[5] N. Hogan, H. I. Krebs, A. Sharon, and J. Charnnarong, "Interactive robotic therapist," Nov. 14 1995, uS Patent 5,466,213.

[6] T. Rahman, W. Sample, and R. Seliktar, "16 design and testing of wrex," in *Advances in rehabilitation robotics*. Springer, 2004, pp. 243–250.

[7] D.-J. Kim, R. Hazlett-Knudsen, H. Culver-Godfrey, G. Rucks, T. Cunningham, D. Portee, J. Bricout, Z. Wang, and A. Behal, "How autonomy impacts performance and satisfaction: Results from a study with spinal cord injured subjects using an assistive robot," *IEEE Transactions on Systems, Man, and Cybernetics-Part A: Systems and Humans*, vol. 42, no. 1, pp. 2–14, 2012.

[8] M. Barsotti, D. Leonardis, C. Loconsole, M. Solazzi, E. Sotgiu, C. Procopio, C. Chisari, M. Bergamasco, and A. Frisoli, "A full upper limb robotic exoskeleton for reaching and grasping rehabilitation triggered by mi-bci," in *2015 IEEE International Conference on Rehabilitation Robotics (ICORR)*. IEEE, 2015, pp. 49–54.

[9] T. B. Pulikottil, M. Caimmi, M. G. D'Angelo, E. Biffi, S. Pellegrinelli, and L. M. Tosatti, "A voice control system for assistive robotic arms: preliminary usability tests on patients," in *2018 7th IEEE International Conference on Biomedical Robotics and Biomechatronics (Biorob)*. IEEE, 2018, pp. 167–172.

[10] E. M. Young, T. J. Withrow, and N. Sarkar, "Design of intention-based assistive robot for upper limb," *Advanced Robotics*, vol. 31, no. 11, pp. 580–594, 2017.

[11] A. Shafti, P. Orlov, and A. A. Faisal, "Gaze-based, context-aware robotic system for assisted reaching and grasping," *arXiv preprint arXiv:1809.08095*, 2018.

[12] A. O. Mohamed, M. P. Da Silva, and V. Courboulay, "A history of eye gaze tracking," 2007.

[13] Y.-M. Jang, R. Mallipeddi, and M. Lee, "Identification of human implicit visual search intention based on eye movement and pupillary analysis," *User Modeling and User-Adapted Interaction*, vol. 24, no. 4, pp. 315–344, 2014.

[14] P. Blignaut, "Fixation identification: The optimum threshold for a dispersion algorithm," *Attention, Perception, & Psychophysics*, vol. 71, no. 4, pp. 881–895, 2009.

[15] D. D. Salvucci and J. H. Goldberg, "Identifying fixations and saccades in eye-tracking protocols," in *Proceedings of the 2000 symposium on Eye tracking research & applications*. ACM, 2000, pp. 71–78.

[16] R. J. Jacob, "Eye tracking in advanced interface design," *Virtual environments and advanced interface design*, pp. 258–288, 1995.

[17] A. Albu-Schaffer, C. Ott, U. Frese, and G. Hirzinger, "Cartesian impedance control of redundant robots: recent results with the dlr-light-weight-arms," in *IEEE International Conference on Robotics and Automation (ICRA)*, 2003, pp. 3704–3709.

[18] P. R. Jones, "Myex: A matlab interface for the tobii eyex eye-tracker," *Journal of Open Research Software*, vol. 6, no. 1, 2018.

[19] M. Quigley, K. Conley, B. Gerkey, J. Faust, T. Foote, J. Leibs, R. Wheeler, and A. Y. Ng, "Ros: an open-source robot operating system," in *ICRA workshop on open source software*, vol. 3, no. 3.2. Kobe, Japan, 2009, p. 5.

[20] S. G. Hart and L. E. Staveland, "Development of nasa-tlx (task load index): Results of empirical and theoretical research," in *Advances in psychology*. Elsevier, 1988, vol. 52, pp. 139–183.

[21] A. Fridlund and J. Cacioppo, "Guidelines for human emg research," *Psychophysiology*, vol. 23, no. 5, pp. 1496–500, 1995.